

---

This is an electronic reprint of the original article.  
This reprint may differ from the original in pagination and typographic detail.

Ceccherini, Sara; Rahikainen, Jenni; Marjamaa, Kaisa; Sawada, Daisuke; Grönqvist, Stina; Maloney, Thaddeus

## Activation of softwood Kraft pulp at high solids content by endoglucanase and lytic polysaccharide monoxygenase

*Published in:*  
Industrial Crops and Products

*DOI:*  
[10.1016/j.indcrop.2021.113463](https://doi.org/10.1016/j.indcrop.2021.113463)

Published: 01/08/2021

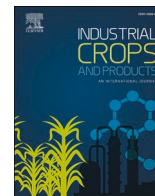
*Document Version*  
Publisher's PDF, also known as Version of record

*Published under the following license:*  
CC BY

*Please cite the original version:*  
Ceccherini, S., Rahikainen, J., Marjamaa, K., Sawada, D., Grönqvist, S., & Maloney, T. (2021). Activation of softwood Kraft pulp at high solids content by endoglucanase and lytic polysaccharide monoxygenase. *Industrial Crops and Products*, 166, Article 113463. <https://doi.org/10.1016/j.indcrop.2021.113463>

---

This material is protected by copyright and other intellectual property rights, and duplication or sale of all or part of any of the repository collections is not permitted, except that material may be duplicated by you for your research use or educational purposes in electronic or print form. You must obtain permission for any other use. Electronic or print copies may not be offered, whether for sale or otherwise to anyone who is not an authorised user.



## Activation of softwood Kraft pulp at high solids content by endoglucanase and lytic polysaccharide monoxygenase

Sara Ceccherini<sup>a,\*</sup>, Jenni Rahikainen<sup>b</sup>, Kaisa Marjamaa<sup>b</sup>, Daisuke Sawada<sup>a</sup>, Stina Grönqvist<sup>b</sup>, Thad Maloney<sup>a</sup>

<sup>a</sup> Department of Bioproducts and Biosystems, Aalto University, P.O. Box 16300, Aalto, Finland

<sup>b</sup> VTT Technical Research Centre of Finland Ltd, Tietotie 2, P.O. Box 1000, FI-02044, VTT, Finland

### ARTICLE INFO

#### Keywords:

Pulp reactivity  
Activation  
Endoglucanase  
Lytic polysaccharide monoxygenase  
LPMO

### ABSTRACT

The manufacturing of man-made cellulose fibers starts with the dissolution of wood pulp fibers. Pulps can dissolve at different rates and leave different amounts of undissolved particles. Thus, their properties can be modified to achieve better dissolution. Enzymatic treatments are an effective means of enhancing pulp dissolution, and this study compares the effect of endoglucanase (TrCel45A) and lytic polysaccharide monoxygenase (LPMO, TrAA9A) on bleached softwood Kraft pulp at 20 % solids content. The enzymes were applied individually and in combination. Both enzymes increased fibrillation, fines content, porosity, water retention value, crystallinity index and crystallite size, but the largest changes were achieved with the enzyme mixture. For example, fiber saturation point and water retention value increased by 64 and 37 % with TrCel45A, by 27 and 25 % with TrAA9A, and by 73 and 52 % with both TrCel45A and TrAA9A. Pulp reactivity was indirectly assessed by measuring the dissolution time in cupriethylenediamine. The average dissolution time of the reference pulp measured 642 s, while those of the pulps treated with TrCel45A, TrAA9A and their mixture were 399, 473 and 298 s, respectively. The decrease in dissolution time correlated with the increase in fines, fibrillation, porosity, and water retention value.

### 1. Introduction

The world population growth and the improvement of the living standards have been rising the demand of several products, such as textiles and clothing (Koszewska, 2018; Michud et al., 2016). The main cellulosic resources for textile production include cotton, jute, and wood fibers. In 2018, cotton accounted for 24.4 % of the global fiber production (Opperskalski et al., 2019). Nevertheless, cotton is poorly sustainable (Shen et al., 2010). It cannot provide for the increasing demand of sustainable textiles, and in the future man-made cellulose fibers are expected to replace part of its current market (Haemmerle, 2011; Michud et al., 2016). From 2014 to 2018, the production of man-made cellulose fibers increased from 5.9 to 6.7 million tons, while the annual growth rate of single viscose and Lyocell fibers between 2017 and 2022 is estimated to be around 7 and 15 %, respectively (Opperskalski et al., 2019).

Man-made cellulose fibers are produced by dissolving high purity wood pulp fibers and then forming and regenerating cellulose into new

filaments. However, the process is hindered by cellulose recalcitrance. The product of cellulose dissolution is a dispersion containing particles of different origins, sizes, and shapes. For instance, viscose dopes can contain mineral, resin-rich, and cellulosic particles and gels with sizes from the nanometer- to the millimeter-scale (Virezub and Pakshver, 1979). Larger particles can be filtered out but they slow down the downstream of the process, while smaller particles pass through the filters and they end up compromising the quality of the regenerated fibers (Treiber, 1981). In view of this, great effort is paid to understand, assess, and improve the reactivity of cellulosic pulp under dissolution.

Pulp reactivity is process specific, and in the viscose process, higher reactivity can correspond to a shorter pre-aging time or to a lower amount of undissolved matter and gel formation (Strunk, 2012). Pulp dissolution can be improved by pretreatments designed to increase the accessibility of the dissolving agents to the reactive groups of cellulose. A higher accessibility generally leads to a better reactivity, and the enhancement of pulp reactivity is called activation. Activation pretreatments can be mechanical, chemical, and/or enzymatic (Shi et al.,

\* Corresponding author at: Department of Bioproducts and Biosystems, Aalto University, Vuorimiehentie 1, 02150, Espoo, Finland.  
E-mail address: [sara.ceccherini@aalto.fi](mailto:sara.ceccherini@aalto.fi) (S. Ceccherini).

<https://doi.org/10.1016/j.indcrop.2021.113463>

Received 13 October 2020; Received in revised form 19 March 2021; Accepted 23 March 2021

Available online 5 April 2021

0926-6690/© 2021 The Author(s). Published by Elsevier B.V. This is an open access article under the CC BY license (<http://creativecommons.org/licenses/by/4.0/>).

2018). Mechanical treatments, such as grinding and refining, can improve pulp reactivity by reducing fibers dimensions and cellulose crystallinity while enhancing fibrillation, surface area, and porosity (Tian et al., 2014; Zhou et al., 2018). Chemical treatments, such as alkali extraction or acid hydrolysis, can be used to increase pulp purity, to optimize the molecular weight distribution, and to modify the crystallinity and the level-off degree of polymerization (Engström et al., 2006; Palme et al., 2016; Wei et al., 1996). Finally, enzymatic treatments can increase pulp porosity, fibrillation and fines content like mechanical treatments, but they can also control the molecular weight distribution or introduce new functional groups like chemical treatments (Duan et al., 2016; Henriksson et al., 2005; Hu et al., 2018; Ibarra et al., 2010; Rahikainen et al., 2019).

The activation achieved with singular mechanical and enzymatic treatments becomes more pronounced when the two treatments are combined, both sequentially (Grönqvist et al., 2014; Miao et al., 2015) or simultaneously (Grönqvist et al., 2015; Rahikainen et al., 2020, 2019). The mechanical action disrupts the fiber structure and therefore it facilitates the adsorption of the enzymes. This synergy is particularly remarkable when pulps are treated at high solids content (Rahikainen et al., 2020). Reducing the water content, the friction between the fibers is increased, and with it also the loosening of the fiber structure and the physical association between enzymes and cellulosic substrate.

Given that cellulose with higher molecular mass fraction is more difficult to dissolve (Kihlman, 2012), enzymes can activate pulp by cellulose depolymerization. Endoglucanases and lytic polysaccharide monoxygenases (LPMOs) can both depolymerize cellulose even if with different mechanisms. The mechanism of endoglucanases is hydrolysis, while LPMOs catalyze an oxidative cleavage which leaves oxidized chain ends to cellulose. Endoglucanases are characterized by a cleft-shaped active site (Davies and Henrissat, 1995). The cleft can accommodate a single polysaccharide chain, which is randomly cleaved. On the contrary, LPMOs have flat substrate-binding surfaces that hydroxylate cellulose at C1 and/or C4. C1 oxidation produces a lactone which is later hydrated into an aldonic acid, while C4 oxidation is suggested to produce a keto-group (Hemsworth et al., 2015). In both cases, the oxidative cleavage of LPMOs requires a co-substrate ( $O_2$  or  $H_2O_2$ ) and an electron donor molecule (e.g. gallic acid) (Forsberg et al., 2019).

It is currently under discussion whether synergy can occur between LPMOs and cellulases (Hansson et al., 2017; Karnaouri et al., 2017; Villares et al., 2017; Zhou et al., 2019). While the hydrolytic action of the endoglucanases is mainly focused on less ordered cellulose (Henriksson et al., 2005; Hu et al., 2018), LPMOs have been reported to oxidize amorphous cellulose, crystalline cellulose and some hemicelluloses (Forsberg et al., 2019; Hansson et al., 2017). The mode of action and the consequent synergy between endoglucanase and LPMO depend on the selected LPMO and substrate. Therefore, a deeper understanding of the interaction between endoglucanase and LPMOs is needed.

To shed more light on the interaction between LPMOs and endoglucanases, this study evaluated the activation of a machine-dried bleached softwood Kraft pulp by means of mechano-enzymatic treatments at high solids content. Two pure monocomponent enzymes were used: endoglucanase TrCel45A and LPMO TrAA9A, both derived from *Trichoderma reesei*. The first hydrolyzes cellulose, while the second performs lytic oxidation at carbon C1 and C4 (Silva et al., 2020). The enzymes were applied and evaluated both singularly and combined. It was hypothesized that the two enzyme families might cooperate synergistically and together achieve a more successful activation of the wood pulp. The variation of pulp reactivity was investigated by means of pulp accessibility and dissolution time.

**Table 1**

List of the acronyms.

Acronym	Meaning
LPMO	Lytic Polysaccharide Monoxygenase
M	Pulp mixed without enzymes
M + TrCel45A	Pulp mixed with endoglucanase
M + TrAA9A	Pulp mixed with LPMO
M + TrCel45A + TrAA9A	Pulp mixed with both endoglucanase and LPMO
WRV	Water Retention Value
FSP	Fiber Saturation Point
[ $\eta$ ]	Intrinsic Viscosity
CHO	Aldehyde Groups
TTC	2,3,5 Triphenyl-2H Tetrazolium Chloride
XRD	X-ray Diffraction
CI	Crystallinity Index
FTIR-ATR	Attenuated Total Reflectance-Fourier Transform Infrared Spectroscopy
LOI	Lateral Order Index
TCI	Total Crystallinity Index
HBI	Hydrogen Bonding Intensity
SEM	Scanning Electron Microscope
CPD	Critical Point Drying
Mw	Weight-average Molecular Weight
DTR	Dissolution-based Torque Reactivity Test
DT	Dissolution Time

## 2. Materials and methods

### 2.1. Pulp

The reference pulp of this work was a machine-dried bleached mixed softwood Kraft pulp (80.4 % cellulose, 9.8 % xylan, 8.9 % glucomannan, 0.9 % lignin) provided by a Finnish pulp mill. It was cold disintegrated according to SCAN-C 18:65, vacuum filtered with a 60  $\mu$ m filter cloth, and homogenized with a Kenwood food mixer with a K-shaped blade.

### 2.2. Enzymes

*Trichoderma reesei* Cel45A endoglucanase was purified from culture supernatant of an engineered *Trichoderma reesei* devoid of major cellulase components Cel7A, Cel6A, Cel7B and Cel5A. The purification was a two-steps procedure employing ion exchange chromatography with DEAE Sepharose FF resin followed by hydrophobic interaction chromatography with Phenyl Sepharose FF resin as described in Karlsson et al. (2002). The *Trichoderma reesei* AA9A LPMO was purified as described in Kont et al. (2019).

### 2.3. Mechano-enzymatic treatments of pulp at high consistency

The treatments were performed at 20 % (w/w) (dry matter) solids content. During the treatments, pH was maintained at 7 using 50 mM sodium phosphate buffer. The treatments were carried out in a SEW Farinograph mixer (Brabender GmbH) at 45 °C and 30 RPM for 5 h. Four samples were produced. The first was mixed without enzymes, while the other three were mixed with endoglucanase, LPMO, and both endoglucanase and LPMO, respectively. The short names of the samples are listed in Table 1.

Enzyme dosage was 0.25 and 0.75 mg protein/g of oven dry pulp for TrCel45A and TrAA9A, respectively. The enzymes were sprayed onto the pulp to promote their homogeneous distribution. When the two enzymes were used together, they were sprayed simultaneously. High purity gallic acid (10 mM) from Sigma-Aldrich (product no. G7384) was

used as an electron donor in the reaction mixture when the LPMO was present. The oxidative action of LPMOs requires an electron donor molecule, and gallic acid has been previously identified as an effective electron donor for LPMOs which does not cleave cellulosic chains when used alone (Kracher et al., 2016).

The treatments were terminated by washing the pulp on a 60  $\mu\text{m}$  filter cloth in a Buchner funnel using  $3 \times 400$  mL deionized water. The first filtrate was re-applied on the pulp to avoid loss of fines. Low amount (0.02 %) of  $\text{NaN}_3$  was applied to the last washing water to preserve the pulp from microbial contamination. The washed pulp was stored in cold (4 °C) prior to analyses.

## 2.4. Sample characterization

### 2.4.1. Assessment of pulp accessibility

**2.4.1.1. Fiber morphology, porosity, and water retention value.** Fines content, fiber length, and fibrillation were measured with a Kajaani FiberLab analyzer. Fiber porosity was analyzed by a two-points solute exclusion technique. Water retention value (WRV), which represents the swelling capacity of a pulp, was measured according to SCAN-C 102 XE.

The two-points solute exclusion technique assesses both the total cell wall pore volume and the micropore volume (diameter  $\leq 3.6$  nm) of pulp fibers (Maloney et al., 1999; Rahikainen et al., 2019). Two 2 wt% dextran solutions were prepared with T2000 and T5 dextrans by Pharmacosmos. Each solution was filtered twice: the first time with a 0.65  $\mu\text{m}$  Millipore filter and the second time with a 0.45  $\mu\text{m}$  Millipore filter. The pulps were adjusted to a solids content of ca.  $20 \pm 1$  %. For each sample, an equivalent of 0.7 g (oven dry basis) pulp and 35 mL dextran solution were placed into a 50 mL disposable centrifuge tube. Thereafter, the tubes were first gently mixed with a rotator for 1 h and then centrifuged in a Thermo Scientific SL40FR centrifuge for 10 min at 3500 g. The supernatant was collected with a syringe and filtered with both a 2  $\mu\text{m}$  and a 0.45  $\mu\text{m}$  filter into the sample holder of an Autopol IV Polarimeter from Rudolph Research. The optical rotation of the dextran solutions and that of the supernatants, i.e. the dextran concentration before and after adding pulp fibers, were measured at 20 °C and at 357 nm wavelength. The total pore volume (fiber saturation point, FSP) and the micropore volume were measured as follows:

$$\text{Volume} = (w_{\text{dex}} + w_{\text{water}}) / w_{\text{pulp}} - (w_{\text{dex}} / w_{\text{pulp}}) \cdot (c_i / c_f)$$

where  $w_{\text{dex}}$ ,  $w_{\text{water}}$  and  $w_{\text{pulp}}$  are the mass of dextran solution (T2000 for FSP and T5 for the micropores), the mass of water in the sample and the bone dry mass of pulp, while  $c_i$  and  $c_f$  are the optical rotations of the dextran solution and of the supernatant, respectively. The measurements were performed in duplicates.

**2.4.1.2. Intrinsic viscosity and molecular weight distribution.** Intrinsic viscosity ( $[\eta]$ ) was measured in duplicates from wet pulps according to standard ISO 5351-1 using a PSL Rheotek equipment (Poulten, Selfe & Lee Ltd, UK). A few copper rods, 25.0 mL of distilled water and ca. 200–250 mg of bone-dry pulp were placed into a plastic bottle and shaken for ca. 30 min. Then, it was added 25.0 mL of cupriethylenediamine, the residual air was squeezed out, and the bottle was shaken for further ca. 30 min. Thereafter, both the bottles and the viscosimeter were adjusted at  $25.0 \pm 0.1$  °C, and finally the efflux time was measured. The viscosity ratio ( $\eta_{\text{rel}}$ ) was calculated multiplying the efflux time by the viscometer constant. In the table provided by the standard,  $\eta_{\text{rel}}$  corresponds to  $\eta_c$ . Finally, intrinsic viscosity was calculated as follows:

$$[\eta] = (\eta_c \cdot w) / d$$

where  $w$  is the bottle weight and  $d$  is the bone-dry mass of pulp.

The molecular weight distribution was determined in duplicates by

size exclusion chromatography with multi-angle light scattering detector. For each sample,  $50 \pm 5$  mg (oven dry basis) of pulp was first soaked two times in 10 mL deionized water for 1 h and then exchanged two times with 8 mL methanol for 45 min followed by two times with 8 mL anhydrous *N,N*-dimethylacetamide (DMAc) for 45 min and ca. 15 h, respectively. In between each step, the sample was filtered under vacuum. After the second exchange with DMAc, the sample and 5.0 mL of 90 g/L LiCl/DMAc were transferred into a glass bottle, where pulp dissolved for 48 h. Finally, a 0.50 mL of dissolved sample was diluted with 4.5 mL of pure DMAc, shaken manually, filtered with a 0.2  $\mu\text{m}$  filter, and analyzed.

**2.4.1.3. Analysis of pulp carbohydrates, solubilized sugars, and pulp aldehydes.** Pulp carbohydrates were quantified according to standard NREL/TP-510-42618 (Sluiter et al., 2012). The monomers were analyzed by high performance anion exchange chromatography with pulsed amperometric detection (HPAEC-PAD) in a Dionex ICS-3000 system, equipped with a CarboPac PA20 column. Cellulose, xylan and glucomannan contents were determined applying the Janson formula (Janson, 1970). The solubilized sugars were analyzed using HPLC as described in Rahikainen et al. (2019).

Pulp aldehydes (CHO groups) were analyzed to verify whether the endoglucanase and the LPMO had a synergistic activity. Some aldehydes are naturally present at the reducing end of cellulose and hemicellulose polymer chains, but their number can be increased by enzyme action. Endoglucanase can increase pulp aldehydes leaving new reducing chain ends after cellulose hydrolysis, while C4-oxidizing LPMOs have been suggested to leave an aldehyde group to the cleaved polymer chain (Hemsworth et al., 2015). Pulp aldehydes were quantified by the Sabolks method. In this method, pulp aldehyde groups reduce 2,3,5 triphenyl-2H tetrazolium chloride (TTC, Sigma-Aldrich) reagent to a red colored formazan which is then quantified with a spectrophotometer (Obolenskaya et al., 1991).

The wet pulp sample (10–15 mg as dry weight) was soaked in 0.5 mL of 0.2 M KOH followed by 5 mL addition of 0.2 % aqueous solution of TTC. The tube was closed, heated for 10 min in a boiling water bath, and then quickly cooled. The tube content was filtered with a glass filter under vacuum into a volumetric tube. The sample was washed on the filter several times with a small amount of ethanol until the pulp became bright again and the filtrate total volume was exactly 10 mL. The absorbance of the filtrate was measured at 546 nm. After boiling, the samples were kept on ice since the colored compound (formazan) is not stable and the color degrades in the course of time. For this reason, all steps of the reaction were completed within 15 min and the time from sample boiling to absorbance measurement was kept constant. A standard curve was constructed using 50  $\mu\text{L}$  of glucose (0.5–4 mg/mL). For calculations, one glucose molecule was considered to contain one aldehyde group that would react in the assay.

**2.4.1.4. Crystallinity and crystallite size.** Crystallinity and crystallite size were assessed by X-ray diffraction and FTIR-ATR spectroscopy, whereof the second provides only relative values (Park et al., 2010) and therefore was used only to validate the diffractometric results.

**2.4.1.4.1. X-ray diffraction (XRD).** XRD data were collected using a SmartLab (RIGAKU) instrument operated at 45 kV and 200 mA ( $\lambda = 1.5418$  Å). The powder samples were first pressed into pellets and then fixed on a sample holder with a transmission geometry. Powder diffraction data were collected in the continuous line scan mode with  $\theta/2\theta$  geometry from 5° to 60°  $2\theta$ . Replicate data were obtained from three different positions in a sample. Air scattering profile without sample was collected under the same experimental condition, and it was subtracted from intensity profiles of samples. The subtracted data were smoothed using Savitzky-Golay filter (Savitzky and Golay, 1964) with a window size of 29 and a polynomial order of 1. The smoothed data were corrected for inelastic scattering.

**Table 2**

Characterization of the main features of the pulp samples. The characterization covers: average fiber length (L), fines content, fibrillation, water retention value (WRV), fiber saturation point (FSP) -representative of the total pore volumes-, micropore volumes, intrinsic viscosity ( $[\eta]$ ), weight-average molecular weight (Mw), aldehydes content (CHO groups), and yield loss.

Sample	A L <sup>a</sup> [mm]	B Fines <sup>a</sup> [%]	C Fibrillation <sup>a</sup> [%]	D WRV [g/g]	E FSP <sup>b</sup> [mL/g]	F Micropores <sup>b</sup> [mL/g]	G [ $\eta$ ] [mL/g]	H Mw [kDa]	I CHO groups [ $\mu$ mol/g]	J Yield Loss [w-%]
Reference	1.90 ± 0.01	3.32 ± 0.01	1.15 ± 0.07	1.22	0.85	0.53	750	731	29 ± 1	–
M	1.60 ± 0.01	5.29 ± 0.03	1.70 ± 0.14	1.39	1.03	0.57	730	–	25 ± 1	0.04
M + TrCel45A	1.27 ± 0.01	6.82 ± 0.14	2.75 ± 0.07	1.67	1.39	0.59	470	654	63 ± 1	0.09
M + TrAA9A	1.46 ± 0.03	5.91 ± 0.03	2.50 ± 0.00	1.52	1.08	0.56	610	725	46 ± 3	0.11
M + TrCel45A + TrAA9A	1.05 ± 0.01	11.25 ± 0.35	3.75 ± 0.07	1.85	1.47	0.62	400	642	84 ± 3	0.33

<sup>a</sup> Measured by Kajaani FiberLab analyzer.

<sup>b</sup> Measured by solute exclusion analysis.

The background profile ( $I_{bkg}(\theta)$ ) was estimated using a smoothing method (Brückner, 2000; Frost et al., 2009) applying Savitzky-Golay filter from 8° to 55° 2 $\theta$  for each diffraction profile. Window size and polynomial order for the Savitzky-Golay filter were set to 201 (corresponding to 4° by 2 $\theta$ ) and 1, respectively. Iteration for the background estimation was repeated 50 times until the iteration reduced the background area significantly. Then the crystallinity index (CI) was estimated using the ratio of the area of total intensity and of the above estimated background intensity from 9° to 50° 2 $\theta$ :

$$CI = 100 * \left( \int I(\theta)d\theta - \int I_{bkg}(\theta)d\theta \right) / \left( \int I(\theta)d\theta \right)$$

The background-corrected profiles in the range from 8° to 26° 2 $\theta$  were fitted with four pseudo-Voigt functions for (1  $\bar{1}$  0), (110), and (200) equatorial diffraction peaks, and a diffraction peak for 102/012 peak. A software LMFIT (Newville et al., 2016) was used for the fitting. Scherrer equation was used to estimate the crystal widths ( $CW_{hkl}$ ) of the lattice planes for cellulose I as follows:

$$CW_{hkl} = K \lambda / \beta_{hkl} \cos\theta$$

where  $K = 0.90$  is the shape factor,  $\lambda$  is the X-ray wavelength,  $\beta_{hkl}$  is the full width at half maximum of the diffraction peak in radians, and  $\theta$  is the diffraction angle of the peak.

**2.4.1.4.2. FTIR-ATR spectroscopy.** FTIR spectra were acquired with a PerkinElmer Spectrum Two FT-IR spectrometer equipped with a Quest attenuated total reflectance attachment and a diamond crystal. The measurements were performed in duplicates within the range 450–4000  $\text{cm}^{-1}$ , with 16 scans, and a resolution of 4  $\text{cm}^{-1}$ . Then, the spectra were normalized at 1336  $\text{cm}^{-1}$  using the PerkinElmer software.

The FTIR-ATR spectra were used to compare the effect of the different treatments on cellulose crystallinity. The literature proposes three standard crystallinity indexes: the total crystallinity index (TCI), the lateral order index (LOI), and the hydrogen bonding intensity (HBI) respectively determined by the ratio between 1373  $\text{cm}^{-1}$  and 2900  $\text{cm}^{-1}$ , 1429  $\text{cm}^{-1}$  and 893  $\text{cm}^{-1}$ , and 3336  $\text{cm}^{-1}$  and 1337  $\text{cm}^{-1}$  (Siroký et al., 2010).

**2.4.1.5. Imaging.** The samples were observed by optical microscope and scanning electron microscope (SEM). For the optical microscope imaging, the samples were first stained with Congo red as in Rahikainen et al. (2019) and then observed with an Olympus BX61 microscope equipped with Olympus WH10X-H-oculars and an Olympus ColorView12-camera using Analysis Pro 3.1-software (Soft Imaging System GmbH). For the SEM imaging, the samples were dried by solvent exchange followed by critical point drying (CPD), sputtered with a 1 nm layer of gold, and imaged with a Zeiss Sigma VP SEM. Solvent exchange and drying were performed as in Lovikka et al. (2016). The CPD was performed with a LEICA EM CPD300 critical point dryer.

#### 2.4.2. Assessment of pulp reactivity

The reactivity of the pulps was assessed by dissolution-based torque reactivity (DTR) test, whose procedure is described elsewhere (Ceccherini and Maloney, 2019). The DTR test provides an indirect estimation of pulp reactivity by monitoring the rheological behavior of the dissolution of pulp fibers in cupriethylenediamine at standard conditions. The dissolution is described by a curve with torque as a function of time. The dissolution rate, the dissolution time (DT), and the final torque plateau provide an indirect evaluation of pulp reactivity; pulps that dissolve faster are considered more reactive. Each sample was tested in triplicate and the average reported.

### 3. Results and discussion

This study evaluates the effect of the mechano-enzymatic treatments with endoglucanase TrCel45A and LPMO TrAA9A on pulp accessibility and reactivity. Pulp accessibility was assessed by measuring pulp porosity, fibrillation, fines content, water retention value, and cellulose crystallinity. Then, it was studied whether the changes at morphological, supramolecular and molecular level had a beneficial effect on the reactivity of the pulp under direct dissolution in cupriethylenediamine.

#### 3.1. Changes in pulp morphology, ultrastructure, and chemistry

##### 3.1.1. Effect of mixing at high consistency

Mixing of pulp at 20 % (w/w) solids content causes friction between the fibers and consequently a mild refining effect (Rahikainen et al., 2020). The loosening and the partial disruption of the cell wall increase cellulose accessibility. In fact, previous studies have demonstrated that when pulp is treated at high consistency, the effect of the endoglucanases is enhanced (Quintana et al., 2015; Rahikainen et al., 2020, 2019).

As shown in Table 2, 5 h mixing at high consistency caused changes at both morphological and ultrastructural level, which led to the rise of the WRV of 0.18 g/g. Pulp fibers were marginally shortened, producing secondary fines. The fines content increased by ca. 2%. The cell wall became partially disrupted and slightly more fibrillated (Fig. 1 (B1–3) and Fig. 2B). The total pore volume (FSP) increased, but without the formation of new micropores. The intrinsic viscosity decreased only slightly, revealing that cellulose DP was almost unaltered. Surprisingly, both XRD and FTIR-ATR reported a decrease in cellulose crystallinity and an increase in crystallite size. Some evaporation can have occurred during 5 h mixing. Thus, the enlargement of the crystallite may have been induced by hornification (Kato and Cameron, 1999).

##### 3.1.2. Effect of the mechano-enzymatic treatments

The mechano-enzymatic treatments combined the mechanical friction of the high consistency mixing with the hydrolytic and oxidative mechanisms of endoglucanase and LPMO, respectively. Their effect was more pronounced than that achieved by mixing pulp at high solids content without enzymes. An overview of the effects of the treatments with TrCel45A, TrAA9A and their combination is shown in Tables 2 and

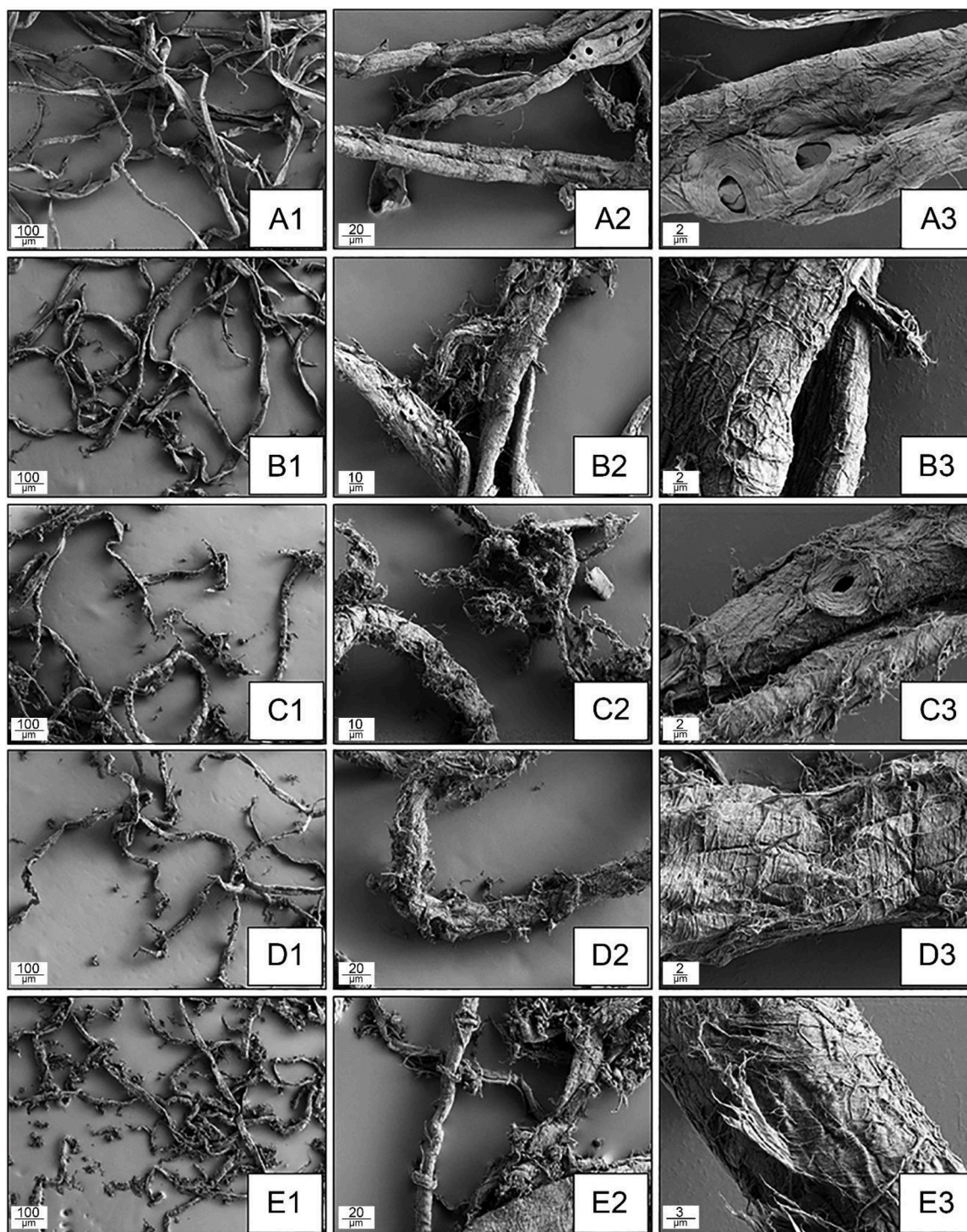


**Fig. 1.** SEM images at increasing magnification. A) Reference pulp. B) Pulp after mixing at high solids content without enzymes. C) Pulp after mixing with TrCel45A. D) Pulp after mixing with TrAA9A. E) Pulp after mixing with TrCel45A and TrAA9A. The numbering refers to the magnification: (1) 100X, (2) 500X, and (3) 2.50KX.

3.

**3.1.2.1. Treatment with endoglucanase (TrCel45A).** The disruptive effect of the mechano-enzymatic treatment with TrCel45A on fiber morphology is visible in Fig. 1 (C1–3) and Fig. 2C. Fines and fibrillation doubled those of the reference (Table 2, B-C), and even though the micropore volumes increased only marginally, the FSP grew by 0.54 mL/g (Table 2, E-F). Hence, compared to mechanical mixing, this treatment had a stronger effect on fibrillation and increased the total

pore volume three times more. The WRV showed a roughly similar increase as the FSP (Table 2, D). The increase in crystallinity (Table 3) supported earlier findings that endoglucanases tend to direct their action onto the less ordered cellulose (Ciolacu and Popa, 2010; Henriksson et al., 2005; Hu et al., 2018), while the larger crystallites concurred with the results published by Hu et al. (2018).

The depolymerization by endoglucanase was confirmed by the production of new C1 reducing ends (aldehyde groups) and by the drop in intrinsic viscosity and Mw respectively by ca. 37 % and 10 % (Table 2, G-

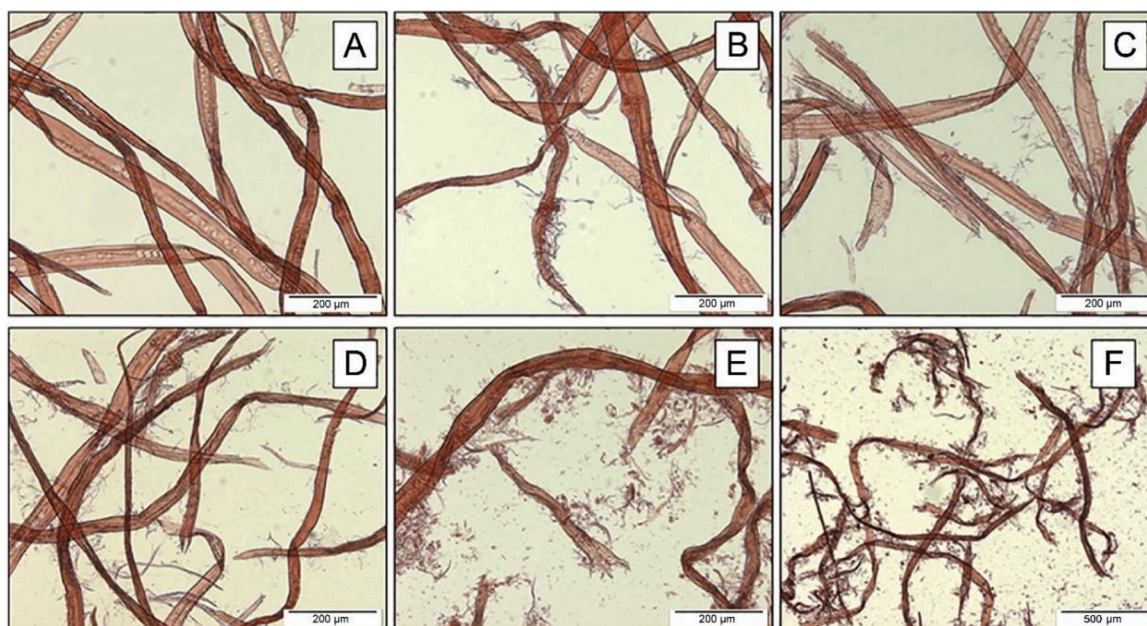


**Fig. 2.** Optical images of the reference pulp (A), the pulp after mixing at high solids content without enzymes (B), the pulp after mixing with TrCel45A (C), the pulp after mixing with TrAA9A (D), and the pulp after mixing with TrCel45A and TrAA9A (E and F).

**Table 3**

Assessment of pulp crystallinity. The characterization covers: crystallinity index (CI), crystallite dimensions (L1m10, L110, and L200) and their average (L avg), lateral order index (LOI), total crystallinity index (TCI) and hydrogen bonding intensity (HBI).

Sample	CI <sup>a</sup> [%]	L1m10 <sup>1</sup> [Å]	L110 <sup>a</sup> [Å]	L200 <sup>a</sup> [Å]	L avg <sup>a</sup> [Å]	LOI <sup>2</sup>	TCI <sup>b</sup>	HBI <sup>b</sup>
Reference	38.6 ± 0.3	31.5 ± 0.5	25.8 ± 0.6	43.7 ± 0.6	33.7 ± 0.6	0.65 ± 0.07	0.40 ± 0.04	6.93 ± 0.91
M	36.8 ± 0.4	34.3 ± 0.7	24.7 ± 0.6	44.5 ± 0.4	34.5 ± 0.5	0.55 ± 0.07	0.37 ± 0.04	6.32 ± 0.42
M + TrCel45A	40.5 ± 0.3	34.5 ± 0.3	33.6 ± 0.9	45.5 ± 0.2	37.9 ± 0.4	0.71 ± 0.04	0.49 ± 0.01	8.09 ± 0.76
M + TrAA9A	38.9 ± 0.4	34.9 ± 0.8	27.0 ± 0.5	45.3 ± 0.2	35.7 ± 0.5	0.68 ± 0.04	0.42 ± 0.00	6.93 ± 0.04
M + TrCel45A + TrAA9A	42.2 ± 0.1	35.5 ± 2.3	33.9 ± 2.3	46.5 ± 2.5	38.6 ± 0.9	0.73 ± 0.02	0.49 ± 0.04	8.85 ± 0.94

<sup>a</sup> Measured by XRD.

<sup>b</sup> Measured by FTIR-ATR.

**Table 4**

Analysis of the solubilized sugars.

Sample	Rhamnose [mg/L]	Arabinose [mg/L]	Galactose [mg/L]	Glucose [mg/L]	Xylose [mg/L]	Mannose [mg/L]	Fructose [mg/L]
Reference	<4	9	11	80	14	4	<4
M + TrCel45A	<4	9	12	234	9	4	<4
M + TrAA9A	<4	11	17	266	40	19	<4
M + TrCel45A + TrAA9A	<4	11	18	942	34	16	<4

D). Despite the degradation, the yield loss measured 0.09 w-% (Table 2, J). Glucose was the only sugar monomer liberated by TrCel45A action (Table 4). Thus, TrCel45A acted primarily on cellulose. These results supported what reported by previous studies (Henriksson et al., 2005; Rahikainen et al., 2019).

**3.1.2.2. Treatment with LPMO (TrAA9A).** The mechano-enzymatic treatment with TrAA9A presented similar but milder effects than the treatment with TrCel45. Fines, fibrillation, crystallinity, and crystallite size were higher than in the sample treated by mixing alone, but lower than in the sample treated with endoglucanase (Fig. 1 (D1–3), Fig. 2D, Tables 2(B–C) and 3). On the other hand, the LPMO had a minor effect on the FSP and no effect on the micropores (Table 2, E–F). Accordingly, TrAA9A increased the WRV but less efficiently than TrCel45A (Table 2, D). These findings differ from those of other studies where LPMOs from *Podospira anserina* were applied on wood pulps at lower solids content (Cathala et al., 2018; Moreau et al., 2019; Villares et al., 2017). In these

studies, it was noticed that the fiber cell wall remained intact unless a second homogenizing step was added. Moreover, crystallinity and crystallite size remained unchanged (Moreau et al., 2019) or were lowered (Villares et al., 2017). It is reasonable that the higher degradation achieved in this study was favored by the combination of the enzymatic action and the mechanical friction due to the mixing at high solids content.

The oxidative depolymerization performed by the LPMO was less powerful than the hydrolytic depolymerization. The intrinsic viscosity decreased by ca. 19 % (Table 2, G) and the Mw remained almost unchanged (Table 2, H). Curiously, the yield loss caused by the LPMO treatment was slightly higher than with the endoglucanase (Table 2, J). A plausible reason could be that the oxidized cello-oligomers generated by LPMO may dissolve more readily than the non-oxidized cello-oligomers generated by the endoglucanase.

Glucose accounted for ca. 75 % of the solubilized sugars, revealing that also TrAA9A acted principally on cellulose (Table 4). The presence of xylose among the other components was attributed to a minor

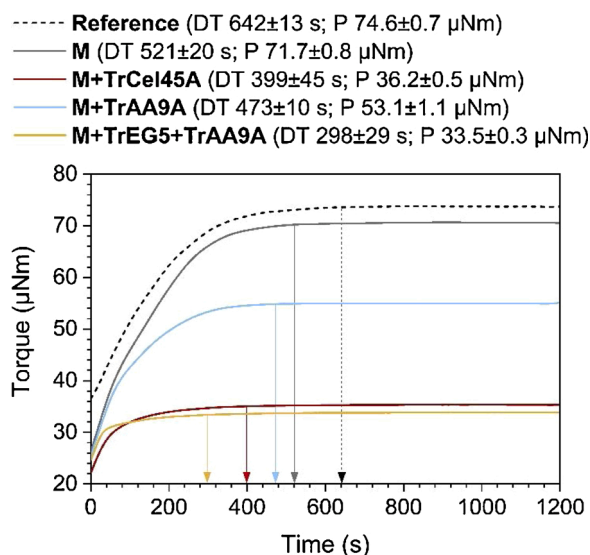


**Fig. 3.** DTR dissolution curves of the reference pulp and of the pulps mixed at high solids content without enzymes (M), with TrCel45A (M + TrCel45A), with TrAA9A (M + TrAA9A), and with TrCel45A and TrAA9A (M + TrCel45A + TrAA9A). The arrows indicate the dissolution time of each curve. The treatments lowered the torque plateau (P) and reduced the dissolution time (DT).

xylanase contamination occurred during the purification of the enzyme. The analysis of the aldehyde (CHO) groups showed an increase of ca. 17  $\mu\text{mol/g}$  compared to the reference pulp (Table 2, I). The additional aldehyde groups in LPMO-treated pulp likely arose from cellulose chain scission due to C4 oxidation. When cellulose chain is cleaved with a C4 oxidative mechanism, a ketoaldose is generated at the non-reducing end, whereas the opposing chain end is left behind as a regular reducing end aldehyde (Hemsworth et al., 2015). This reducing end aldehyde is likely detected with the TTC assay.

**3.1.2.3. Treatment with TrCel45A and TrAA9A.** The pulp treated with both TrCel45A and TrAA9A showed the most severe changes. Compared to the reference, the fibrillation was three times higher, while the average fiber length was almost halved, causing the rise of the fine content by ca. 8 % (Table 2, A-C). The FSP was ca. 73 % higher than in the reference, ca. 43 % higher than in the sample mixed with no enzymes, and it included new micropores (Table 2, E-F). Of the enzymes used singularly, only the endoglucanase produced new micropores, and the increase was by ca. 3 %. Here, using both the enzymes together, the

micropores increased by ca. 8 %. The growth in fines, fibrillation, and porosity affected the WRV, which was higher than the reference by ca. 52 % (Table 2, D). It is plausible that the swelling produced by the LPMO allowed a deeper penetration of the endoglucanase and consequently a more aggressive hydrolytic action.

The increase in crystallinity and crystallite size (Table 3) seems somewhat contradictory to the increase in WRV, because a higher order at supramolecular level is usually associated with a lower accessibility (Ciolacu and Popa, 2010). The ultrastructure changed more when the enzymes were used together. It is possible that these changes were mainly driven by the endoglucanase. However, the action of the endoglucanase grew with its further penetration in the cell wall promoted by the LPMO. Hu et al. (2018) reported the same trends but with more drastic changes. The crystallinity and the crystallite size were increased by 14 % and 52 % using endoglucanase and by 18 % and 60 % using endoglucanase with LPMO. In the present study, the same features increased by 5 % and 12 % using TrCel45A and by 9 % and 14 % using TrCel45A with TrAA9A. The higher crystallinity achieved using the enzymes together was explained by Hu and coauthors as the result of an enhanced intermolecular hydrogen bonding network due to the conversion of the carbonyl groups on the ketone structure into 4-ketoaldoses (gem-diol) groups after C4 oxidation.

Confirming previous results (Hu et al., 2018), the simultaneous occurrence of the hydrolytic and oxidative mechanisms led to a more effective depolymerization, which is visible in the higher yield loss and in the lower intrinsic viscosity and Mw (Table 2, G-H). However, it is unclear whether endoglucanase and LPMO acted synergistically or additively. The solubilized sugars seem to indicate a synergistic interaction, because the amount of glucose released by the enzyme mixture was significantly higher than the sum of the glucose released by endoglucanase and LPMO individually (Table 4). On the other hand, the aldehyde groups denote an additive behavior, because the amount of reducing end aldehydes produced by the enzyme mixture (55  $\mu\text{mol/g}$ ) was only slightly higher than the sum of those produced by the single enzymes (34 + 17 = 51  $\mu\text{mol/g}$ ).

### 3.2. Changes in pulp reactivity

The changes that the treatments induced to the chemistry, the ultrastructure, and the morphology of the pulp contributed to improve its accessibility and consequently its reactivity under dissolution. The ease of dissolution was assessed by the DTR test, which monitors the rheological behavior of pulp dissolution in cupriethylenediamine at standard conditions (Ceccherini and Maloney, 2019). The principal outcome is the dissolution time (DT), which is the interval from the injection of the solvent and the stabilization of the torque plateau. The second outcome

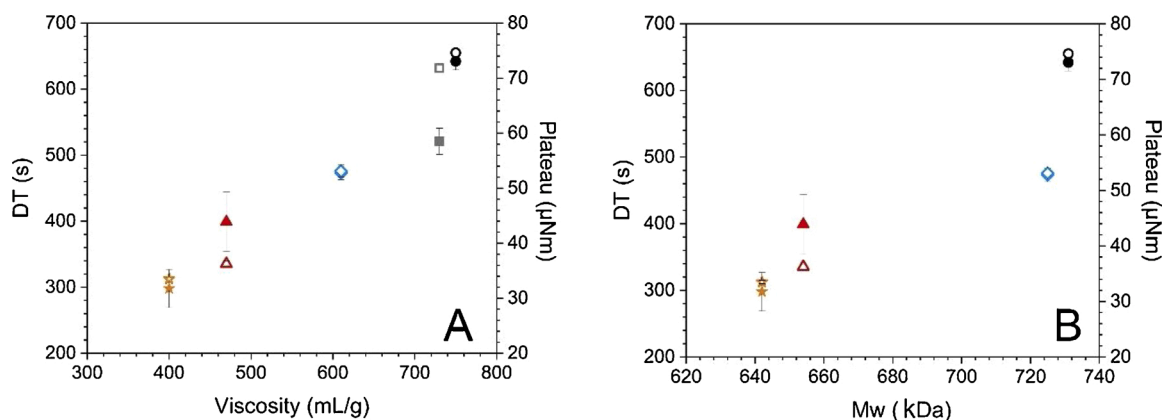


**Fig. 4.** Variation of dissolution time (full symbols) and torque plateau (open symbols) as a function of intrinsic viscosity (A) and Mw (B). The color and the shape of the symbols indicate the sample: black circle for the reference, gray square for M, red triangle for M + TrCel45A, blue diamond for M + TrAA9A and yellow star for M + TrCel45A + TrAA9A.

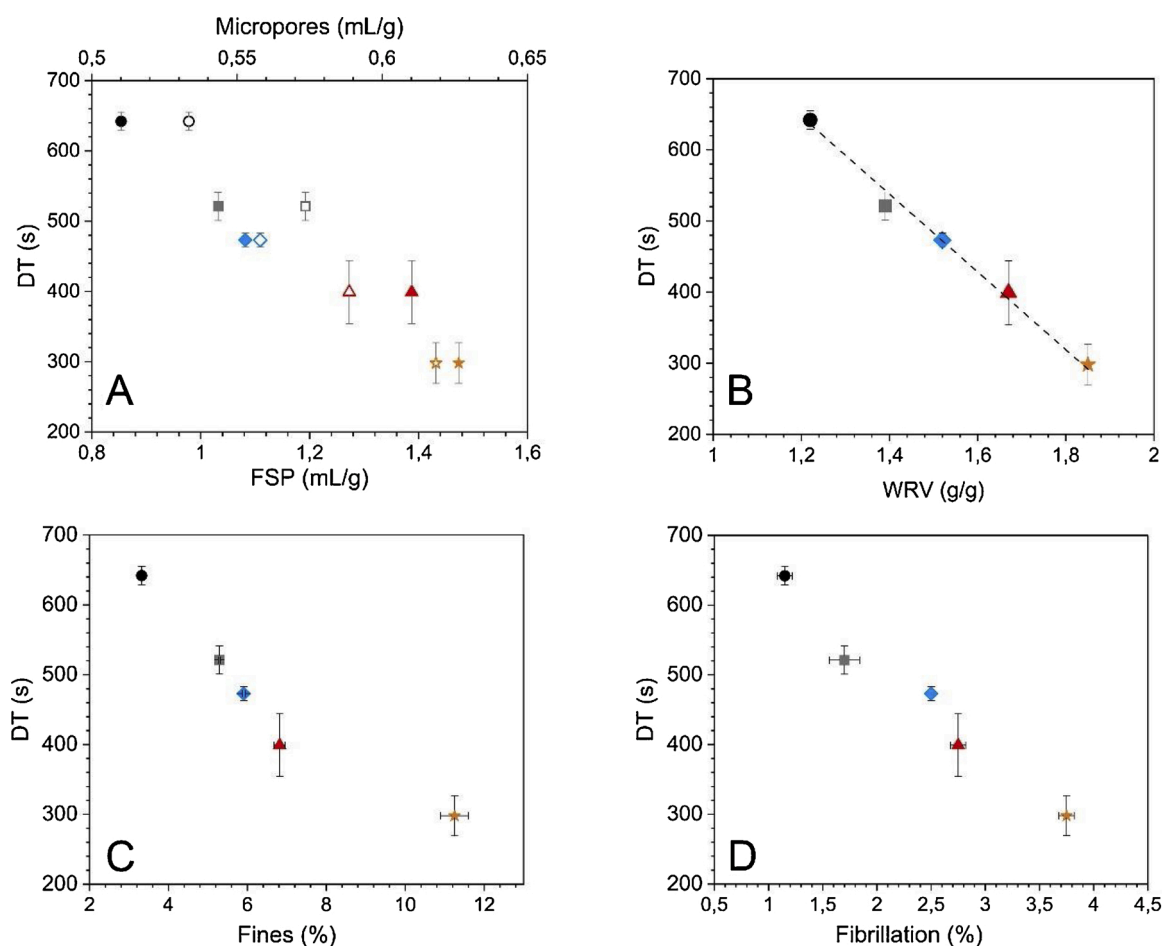


**Fig. 5.** Variation of dissolution time as a function of (A) fiber saturation point (full symbols) and micropores (open symbols), (B) water retention value, (C) fines, and (D) fibrillation. The color and the shape of the symbols indicate the sample: black circle for the reference, gray square for M, red triangle for M + TrCel45A, blue diamond for M + TrAA9A and yellow star for M + TrCel45A + TrAA9A.

is the torque plateau itself.

According to the DTR test, the treatments activated the pulp to different extents (Fig. 3). All the treated samples had lower torque plateaus and shorter dissolution times than the reference, but the two parameters were not proportional to each other. The plateau values were mainly driven by viscosity and consequently by the degree of polymerization, while the dissolution time was simultaneously affected by all the morphological, molecular, and supramolecular features of the pulp.

The 5 h mixing at high solids content reduced the dissolution time by almost 20 %. However, the combination of the high consistency mixing with the hydrolytic and oxidative mechanisms of endoglucanase and LPMO shortened the dissolution even further. The TrCel45A proved more effective than the TrAA9A, and the shortest dissolution time was achieved treating the pulp with both endoglucanase and LPMO. The treatments with TrCel45A, TrAA9A and their mixture decreased the dissolution time by 38, 26 and 53 %, respectively. The dissolution became faster with the shortening of cellulose chains and the increase in fines, fibrillation, porosity (both meso- and micropores) and swelling produced by the treatments (Figs. 4 and 5), even if these increased also the crystallinity and the crystallite size. Considering that all these properties were maximized when TrCel45A and TrAA9A were used together, this treatment led to the fastest dissolution.

#### 4. Conclusions

The mechano-enzymatic treatments accelerated pulp dissolution

integrating the effects of hydrolytic and/or oxidizing depolymerization to the mild refining action of mixing at high solids content. TrCel45A and TrAA9A increased pulp crystallinity index and cellulose crystallite size, but they also increased the fines, fibrillation, FSP, and WRV already improved by mixing alone. However, TrAA9A had no effect on pulp micropores, and its changes were less pronounced than those of TrCel45A.

The morphological and molecular changes were greatest when TrCel45A and TrAA9A were used together. The solubilized sugars might suggest that endoglucanase and LPMO acted synergistically, while the reducing end aldehydes and the molecular and morphological features indicate that the positive effect was the result of an additive behavior. The pulp treated with both TrCel45A and TrAA9A was the fastest to dissolve.

This study focused on dissolution time, which is one important aspect of pulp reactivity. Future studies could also consider the amount and type of undissolved material which is also relevant.

#### Credit author statement

The study was conceived and designed by **Sara Ceccherini, Jenni Rahikainen, Kaisa Marjamaa, Stina Grönqvist and Thad Maloney**. **Jenni Rahikainen, Kaisa Marjamaa and Stina Grönqvist** prepared the samples and performed the following analyses: intrinsic viscosity, solubilized sugars and aldehydes quantification and imaging by optical microscope. **Sara Ceccherini and Thad Maloney** performed the following analyses: fiber morphology, porosimetry, water retention

value, imaging by SEM, molecular weight, quantification of pulp carbohydrates, FT-IR spectroscopy and assessment of pulp reactivity. **Daisuke Sawada** measured the samples by X-ray diffraction. **Sara Ceccherini** wrote the manuscript. All authors approved the final version of the manuscript.

### Declaration of Competing Interest

The authors declare that they have no known competing financial interests or personal relationships that could have appeared to influence the work reported in this paper.

### Acknowledgments

The authors acknowledge the funding support by the Academy of Finland (grants n:o 277791 and 279255) for the project "Development of porosity at high solids loading in the early stages of fibre treatment by cellulose-active enzymes". The work of VTT was partially done in CLIC Innovation project NewFP funded by Business Finland. In addition, we are grateful for the support provided by the FinnCERES Materials Bioeconomy Ecosystem (Academy of Finland), Aalto University, and the Finnish Association of Forest Products Engineers (Puunjalostusinsinööritry).

### Appendix A. Supplementary data

Supplementary material related to this article can be found, in the online version, at doi:<https://doi.org/10.1016/j.indcrop.2021.113463>.

### References

- Brückner, S., 2000. Estimation of the background in powder diffraction patterns through a robust smoothing procedure. *J. Appl. Crystallogr.* 33, 977–979. <https://doi.org/10.1107/S0021889800003617>.
- Cathala, B., Villares, A., Berrin, J.-G., Moreau, C., 2018. Method for Producing Nanocellulose From a Cellulose Substrate. US 2018 / 0142084 A1.
- Ceccherini, S., Maloney, T., 2019. Assessing wood pulp reactivity through its rheological behavior under dissolution. *Cellulose* 26, 9877–9888. <https://doi.org/10.1007/s10570-019-02750-0>.
- Ciolacu, D., Popa, V.I., 2010. Reactivity of cellulose. *Cellulose Allomorphs: Structure, Accessibility and Reactivity*. Nova Science Publishers, New York, pp. 43–45.
- Davies, G., Henrissat, B., 1995. Structures and mechanisms of glycosyl hydrolases. *Structure* 3, 853–859.
- Duan, C., Verma, S.K., Li, J., Ma, X., Ni, Y., 2016. Viscosity control and reactivity improvements of cellulose fibers by cellulase treatment. *Cellulose* 23, 269–276. <https://doi.org/10.1007/s10570-015-0822-9>.
- Engström, A., Ek, M., Henriksson, G., 2006. Improved Accessibility and Reactivity of Dissolving Pulp for the Viscose Process : Pretreatment with Monocomponent Endoglucanase. *Biomacromolecules* 7, 2027–2031.
- Forsberg, Z., Sørle, M., Petrović, D., Courtade, G., Aachmann, F.L., Vaaje-Kolstad, G., Bissaro, B., Rohr, Å.K., Eijsink, V.G., 2019. Polysaccharide degradation by lytic polysaccharide monoxygenases. *Curr. Opin. Struct. Biol.* 59, 54–64. <https://doi.org/10.1016/j.sbi.2019.02.015>.
- Frost, K., Kaminski, D., Kirwan, G., Lascaris, E., Shanks, R., 2009. Crystallinity and structure of starch using wide angle X-ray scattering. *Carbohydr. Polym.* 78, 543–548. <https://doi.org/10.1016/j.carbpol.2009.05.018>.
- Grönqvist, S., Hakala, T.K., Kampuri, T., Vehviläinen, M., Hänninen, T., Liitiä, T., Maloney, T., Suurnäkki, A., 2014. Fibre porosity development of dissolving pulp during mechanical and enzymatic processing. *Cellulose* 21, 3667–3676. <https://doi.org/10.1007/s10570-014-0352-x>.
- Grönqvist, S., Kampuri, T., Maloney, T., Vehviläinen, M., Liitiä, T., Suurnäkki, A., 2015. Enhanced pre-treatment of cellulose pulp prior to dissolution into NaOH/ZnO. *Cellulose* 22, 3981–3990. <https://doi.org/10.1007/s10570-015-0742-8>.
- Haemmerle, F.M., 2011. The cellulose gap (The future of cellulosic fibres). *Lenzinger Berichte* 89, 99–100.
- Hansson, H., Karkehabadi, S., Mikkelsen, N., Douglas, N.R., Kim, S., Lam, A., Kaper, T., Kelemen, B., Meier, K.K., Jones, S.M., Solomon, E.I., Sandgren, M., 2017. High-resolution structure of a lytic polysaccharide monoxygenase from *Hypocrea jecorina* reveals a predicted linker as an integral part of the catalytic domain. *J. Biol. Chem.* 292, 19099–19109. <https://doi.org/10.1074/jbc.M117.799767>.
- Hemsworth, G.R., Johnston, E.M., Davies, G.J., Walton, P.H., 2015. Lytic polysaccharide monoxygenases in biomass conversion. *Trends Biotechnol.* 33, 747–761. <https://doi.org/10.1016/j.tibtech.2015.09.006>.
- Henriksson, G., Christiernin, M., Agnemo, R., 2005. Monocomponent endoglucanase treatment increases the reactivity of softwood sulphite dissolving pulp. *J. Ind. Microbiol. Biotechnol.* 32, 211–214. <https://doi.org/10.1007/s10295-005-0220-7>.
- Hu, J., Tian, D., Renneckar, S., Saddler, J.N., 2018. Enzyme mediated nanofibrillation of cellulose by the synergistic actions of an endoglucanase, lytic polysaccharide monoxygenase (LPMO) and xylanase. *Sci. Rep.* 8, 4–11. <https://doi.org/10.1038/s41598-018-21016-6>.
- Ibarra, D., Köpcke, V., Ek, M., 2010. Behavior of different monocomponent endoglucanases on the accessibility and reactivity of dissolving-grade pulps for viscose process. *Enzyme Microb. Technol.* 47, 355–362. <https://doi.org/10.1016/j.enzmictec.2010.07.016>.
- Janson, J., 1970. Calculation of the polysaccharide composition of wood and pulp. *Pap. ja puu* 52, 323–329.
- Karlsson, J., Siika-aho, M., Tenkanen, M., Tjerneld, F., 2002. Enzymatic properties of the low molecular mass endoglucanases Cel12A (EG III) and Cel45A (EG V) of *Trichoderma reesei*. *J. Biotechnol.* 99, 63–78.
- Karnaouri, A., Muraleedharan, M.N., Dimarogona, M., Topakas, E., Rova, U., Sandgren, M., Christakopoulos, P., 2017. Recombinant expression of thermostable processive MTEG5 endoglucanase and its synergism with MLEPMO from *Myceliophthora thermophila* during the hydrolysis of lignocellulosic substrates. *Biotechnol. Biofuels* 10. <https://doi.org/10.1186/s13068-017-0813-1>.
- Kato, K.L., Cameron, R.E., 1999. A review of the relationship between thermally-accelerated ageing of paper and hornification. *Cellulose* 6, 23–40. <https://doi.org/10.1023/A:1009292120151>.
- Kihlman, M., 2012. Dissolution of Cellulose for Textile Fibre Applications. Karlstad University.
- Kont, R., Pihlajaniemi, V., Borisova, A.S., Aro, N., Marjamaa, K., Loogen, J., Büchs, J., Eijsink, V.G.H., Kruus, K., Våljamäe, P., 2019. The liquid fraction from hydrothermal pretreatment of wheat straw provides lytic polysaccharide monoxygenases with both electrons and H<sub>2</sub>O<sub>2</sub> co-substrate. *Biotechnol. Biofuels* 12. <https://doi.org/10.1186/s13068-019-1578-5>.
- Koszevska, M., 2018. Circular economy - challenges for the textile and clothing industry. *Autex Res. J.* 18, 337–347. <https://doi.org/10.1515/aut-2018-0023>.
- Kracher, D., Scheiblbrandner, S., Felice, A.K.G., Breslmayr, E., Preims, M., Ludwicka, K., Haltrich, D., Eijsink, V.G.H., Ludwig, R., 2016. Extracellular electron transfer systems fuel cellulose oxidative degradation. *Science* (80-) 352, 1098–1101. <https://doi.org/10.1126/science.aaf3165>.
- Lovikka, V.A., Khanjani, P., Väisänen, S., Vuorinen, T., Maloney, T.C., 2016. Porosity of wood pulp fibers in the wet and highly open dry state. *Microporous Mesoporous Mater.* 234, 326–335. <https://doi.org/10.1016/j.micromeso.2016.07.032>.
- Maloney, T.C., Laine, J., Paulapuro, H., 1999. Comments on the measurement of cell wall water. *Tappi J.* 82, 125–127.
- Miao, Q., Tian, C., Chen, L., Huang, L., Zheng, L., Ni, Y., 2015. Combined mechanical and enzymatic treatments for improving the Fock reactivity of hardwood kraft-based dissolving pulp. *Cellulose* 22, 803–809. <https://doi.org/10.1007/s10570-014-0495-9>.
- Michud, A., Tantt, M., Asaadi, S., Ma, Y., Persson, A., Netti, E., Ka, P., Berntsson, A., Hummel, M., Sixta, H., 2016. Ioncell-F : ionic liquid-based cellulosic textile fibers as an alternative to viscose and Lyocell. *Text. Res. J.* 86, 543–552. <https://doi.org/10.1177/0040517515591774>.
- Moreau, C., Tapin-Lingua, S., Grisel, S., Gimbert, I., Le Gall, S., Meyer, V., Petit-Conil, M., Berrin, J.G., Cathala, B., Villares, A., 2019. Lytic polysaccharide monoxygenases (LPMOs) facilitate cellulose nanofibrils production. *Biotechnol. Biofuels* 12, 13–17. <https://doi.org/10.1186/s13068-019-1501-0>.
- Newville, M., Stensitzki, T., Allen, D.B., Rawlik, M., Ingargiola, A., Nelson, A., 2016. LMFIT: non-linear least-square minimization and curve-fitting for Python. *Astrophys. Source Code Libr.* <https://doi.org/10.5281/ZENODO.11813>.
- Obolenskaya, A.V., Yelnitskaya, Z.P., Leonovitch, A.A., 1991. Laboratory studies of wood and cellulose chemistry. *Ekologiya. Moscow*.
- Opperskalski, S., Siew, S., Tan, E., Truscott, L., 2019. Preferred Fiber & Materials Market Report 2019.
- Palme, A., Theliander, H., Breid, H., 2016. Acid hydrolysis of cellulosic fibres: comparison of bleached kraft pulp, dissolving pulps and cotton textile cellulose. *Carbohydr. Polym.* 136. <https://doi.org/10.1016/j.carbpol.2015.10.015>.
- Park, S., Baker, J.O., Himmel, M.E., Parilla, P.A., Johnson, D.K., 2010. Cellulose crystallinity index: measurement techniques and their impact on interpreting cellulase performance. *Biotechnol. Biofuels* 3, 10. <https://doi.org/10.1186/1754-6834-3-10>.
- Quintana, E., Valls, C., Vidal, T., Roncero, M.B., 2015. Comparative evaluation of the action of two different endoglucanases. Part I: on a fully bleached, commercial acid sulfite dissolving pulp. *Cellulose* 22, 2067–2079. <https://doi.org/10.1007/s10570-015-0623-1>.
- Rahikainen, J., Ceccherini, S., Molinier, M., Holopainen-Mantila, U., Reza, M., Väisänen, S., Puranen, T., Kruus, K., Vuorinen, T., Maloney, T., Suurnäkki, A., Grönqvist, S., 2019. Effect of cellulase family and structure on modification of wood fibres at high consistency. *Cellulose* 26, 5085–5103. <https://doi.org/10.1007/s10570-019-02424-x>.
- Rahikainen, J., Mattila, O., Maloney, T., Lovikka, V., Kruus, K., Suurnäkki, A., Grönqvist, S., 2020. High consistency mechano-enzymatic pretreatment for kraft fibres: effect of treatment consistency on fibre properties. *Cellulose* 27, 5311–5322. <https://doi.org/10.1007/s10570-020-03123-8>.
- Savitzky, A., Golay, M.J.E., 1964. Smoothing and differentiation of data by simplified least squares procedures. *Anal. Chem.* 36, 1627–1639. <https://doi.org/10.1021/ac60214a047>.
- Shen, L., Worrell, E., Patel, M.K., 2010. Environmental impact assessment of man-made cellulose fibres. *Resour. Conserv. Recycl.* 55, 260–274. <https://doi.org/10.1016/j.resconrec.2010.10.001>.
- Shi, Z., Liu, Y., Xu, H., Yang, Q., Xiong, C., Kuga, S., Matsumoto, Y., 2018. Facile dissolution of wood pulp in aqueous NaOH/urea solution by ball milling

- pretreatment. *Ind. Crops Prod.* 118, 48–52. <https://doi.org/10.1016/j.indcrop.2018.03.035>.
- Silva, C., Teixeira, T., Rodrigues, K., A.S.-A., 2020. U., 2020. Combination of MALDI-TOF MS and UHPLC-ESI-MS for the characterization of lytic polysaccharide monoxygenase activity. *Anal. Methods* 12, 149–161.
- Široký, J., Blackburn, R.S., Bechtold, T., Taylor, J., White, P., 2010. Attenuated total reflectance Fourier-transform Infrared spectroscopy analysis of crystallinity changes in lyocell following continuous treatment with sodium hydroxide. *Cellulose* 17, 103–115. <https://doi.org/10.1007/s10570-009-9378-x>.
- Sluiter, A., Hames, B., Ruiz, R., Scarlata, C., Sluiter, J., Templeton, D., Crocker, D., 2012. NREL/TP-510-42618 analytical procedure - Determination of structural carbohydrates and lignin in Biomass. *Lab. Anal. Proced.* 17 <https://doi.org/NREL/TP-510-42618>.
- Strunk, P., 2012. Characterization of Cellulose Pulps and the Influence of Their Properties on the Process and Production of Viscose and Cellulose Ethers. Umeå University.
- Tian, C., Zheng, L., Miao, Q., Cao, C., Ni, Y., 2014. Improving the reactivity of kraft-based dissolving pulp for viscose rayon production by mechanical treatments. *Cellulose* 21, 3647–3654. <https://doi.org/10.1007/s10570-014-0332-1>.
- Treiber, E., 1981. Cleanness problem for viscose spinning solutions. *Ind. Eng. Chem. Prod. Res. Dev.* 20, 231–237. <https://doi.org/10.1021/i300002a005>.
- Villares, A., Moreau, C., Bennati-Granier, C., Garajova, S., Foucat, L., Falourd, X., Saake, B., Berrin, J.-G., Cathala, B., 2017. Lytic polysaccharide monoxygenases disrupt the cellulose fibers structure. *Sci. Rep.* 7, 40262. <https://doi.org/10.1038/srep40262>.
- Virezub, A.I., Pakshver, A.B., 1979. Viscose filtration (review). *Fibre Chem.* 10, 246–254. <https://doi.org/10.1007/BF00545113>.
- Wei, S., Kumar, V., Banker, G.S., 1996. Phosphoric acid mediated depolymerization and decrystallization of cellulose: preparation of low crystallinity cellulose - A new pharmaceutical excipient. *Int. J. Pharm.* 142, 175–181. [https://doi.org/10.1016/0378-5173\(96\)04673-X](https://doi.org/10.1016/0378-5173(96)04673-X).
- Zhou, S., Li, Y., Huang, L., Chen, L., Miao, Q., 2018. Enhanced reactivity of kraft-based viscose-grade dissolving pulp by hollander beating treatment. *BioResources* 13, 2861–2870. <https://doi.org/10.15376/biores.13.2.2861-2870>.
- Zhou, H., Li, T., Yu, Z., Ju, J., Zhang, H., Tan, H., Li, K., Yin, H., 2019. A lytic polysaccharide monoxygenase from *Myceliophthora thermophila* and its synergism with cellobiohydrolases in cellulose hydrolysis. *Int. J. Biol. Macromol.* 139, 570–576. <https://doi.org/10.1016/j.ijbiomac.2019.08.004>.